Electronic Supplementary Material (ESI) for Physical Chemistry Chemical Physics.

Supporting Information

Vacancy-Induced MnO_6 Distortion and Its Impacts on Structural Transition of Li_2MnO_3

Yurui Gao[abd], Jun Ma[abc], Zhaoxiang Wang*[ab], Gang Lu[d], Liquan Chen[ab]

[a] Key Laboratory for Renewable Energy, Chinese Academy of Sciences, Beijing Key Laboratory for New Energy Materials and Devices, Beijing National Laboratory for Condensed Matter Physics, Institute of Physics, Chinese Academy of Sciences, P O Box 603, Beijing 100190, China

** Corresponding author. E-mail: zxwang@iphy.ac.cn (Z. X. Wang).*

Tel.: +86 10 82649047. fax: +86 10 82649050.

[b] School of Physical Sciences, University of Chinese Academy of Sciences, Beijing 100190, China

[c] Qingdao Industrial Energy Storage Technology Institute, Qingdao Institute of Bioenergy and Bioprocess Technology, Chinese Academy of Sciences, Qingdao 266101, China

[d] Department of Physics and Astronomy, California State University Northridge, Northridge, California 91330-8268, USA

1. Simulation temperature

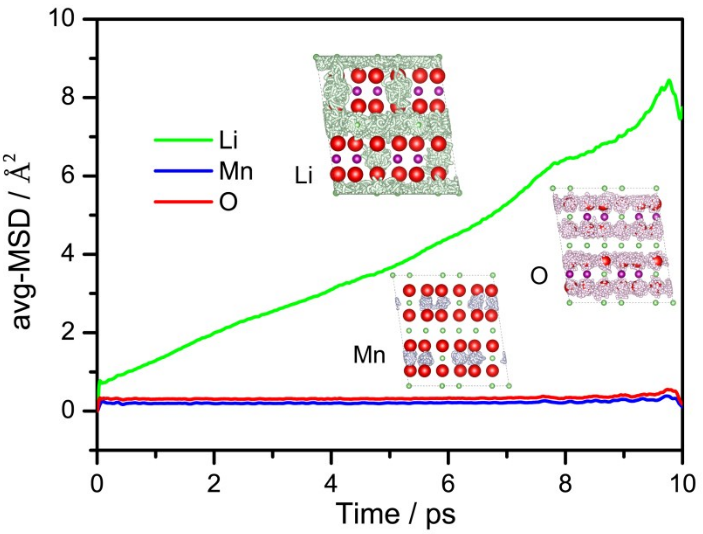

Fig. 1S MSDs and trajectories of atoms in a perfect Li_2MnO_3 with U_{eff}=4.9 eV at 3000K.

As can be seen from Fig. 1S, in the perfect Li_2MnO_3, Mn and O atoms vibrate around their equilibrium positions up to a simulation temperature of 3000 K. At this temperature, it is found that only Li atoms diffuse, in agreement with Xiao's report.[1] In order to increase the efficiency, the FPMD simulation is performed at 3000 K in the article.

2. Bader charge and net spin analysis

Bader analysis is firstly conducted in order to study the charge reorganization during the Mn migration. Table 1S shows the Bader atomic charge of the migrating Mn in each snapshot shown in Fig.3 (from *a* to *i*). The initial Bader charge of the migrating Mn is +2.102. When it migrates, its Bader charge decreases and fluctuates, probably due to the octahedral distortion, atomic coordination and atomic vibration deviation. When Mn migrates into the octahedral site in the Li layer, its Bader charge recovers to +1.933, 0.169 e lower than the initial charge.

Table 1S. Bader atomic charge (e) of the migrating Mn in each snapshot in Fig.3 (from *a* to *i*).

a	*b*	*c*	*d*	*e*	*f*	*g*	*h*	*i*
+2.102	+1.748	+1.788	+1.789	+1.653	+1.710	+1.470	+1.574	+1.933

To be more specific, the net up spin of the migrating Mn is then plotted in Fig. 2S. In the initial V_O-Li_2MnO_3 (snapshot *a* in Fig. 3), Mn has the electron configuration of $3d^3$ and is +4 in valence. The net spin of Mn increases, revealing its reduction from +4 to +3 ($3d^4$) and even +2 ($3d^5$) as it migrates. Moreover, the valence of Mn fluctuates during migration, in agreement with the above Bader charge analysis. Finally, when Mn enters the octahedral site in the Li layer, its valence becomes +3.

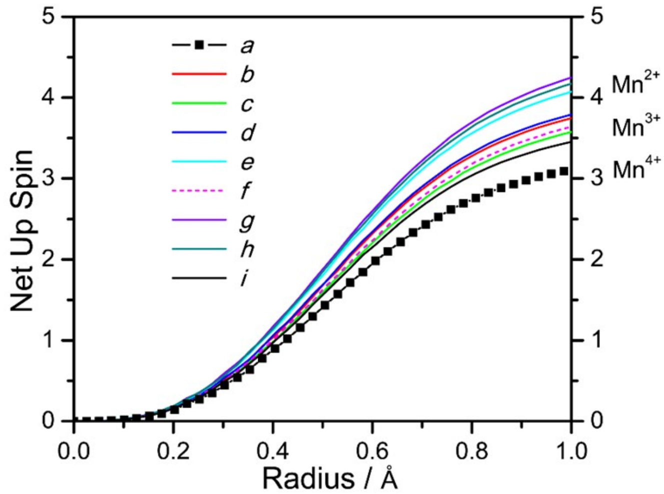

Fig. 2S The net spin of the migrating Mn. The valences are calibrated with Li_2MnO_2, $LiMnO_2$ and Li_2MnO_3 shown in Fig. 3S d.

In order to examine the charge transfer as Mn migrates, three configurations were relaxed: (1) the first/initial configuration (snapshot *a*); (2) the intermediate configuration with Mn at the tetrahedral site in the Li layer (snapshot *f*); (3) the last configurations (snapshot *i*). Then, we carefully examined the net spin charge of all the Mn ions and the Bader charge of all the O ions in these configurations (Fig. 3S). For snapshot *a*, the presence of one O vacancy results in two Mn^{3+} ions while the valence of the migrating Mn is +4. As Mn migrates to the tetrahedral site (snapshot *f*), one O-O bond is formed. The valence of the migrating Mn decreases from Mn^{4+} to Mn^{3+}, with the presence of another Mn^{3+}. Meanwhile, the Bader charge around O increases, mainly on the two O atoms on the O-O bond. As for snapshot *i*, Mn stays on the octahedral site in the Li layer with the valence of +3. Besides, the other Mn^{3+} ion other than the two originally induced by V_O stays in the TM-layer octahedron sharing one O atom with the MnO_6 octahedron in the Li layer. They form the spinel nucleus. Again, the simulation of the Bader charge distribution shows that the charge is mainly transferred from the O atoms on the O-O bond to Mn. The configuration of snapshot *h* is also relaxed. But the coordination number (CN=4) of the migrating Mn in this configuration is not stable in thermodynamics: the tetrahedral Mn reaches the octahedral site after relaxation. The variable distribution of O Bader charge (h in Fig. 3S) shows that more electrons are transferred from the O-O bond to the migrating Mn ion, rendering its valence +2 displayed by its net spin (Fig. 2S).

According to the above discussion, two possible processes can be deduced during Mn migration in Li_2MnO_3:

$$2Mn^{4+} + 2O^{2-} = 2Mn^{3+} + (O_2)^{2-}$$

and

$$Mn^{4+} + 2O^{2-} = Mn^{2+} + (O_2)^{2-}$$

Therefore, the Mn acquires electrons from O as Mn migration and its valence decreases. Probably due to the MnO_6 distortion and atomic coordination, the distribution of the two electrons mainly lost from the O atoms on the O-O bond experiences a series of adjustments to form two Mn^{3+} or one Mn^{2+} during Mn migration. As Mn enters the octahedral site in the Li layer, its valence becomes Mn^{3+}, with the presence of one neighboring Mn^{3+} in the TM layer sharing one O atom with it, forming the spinel nucleus.

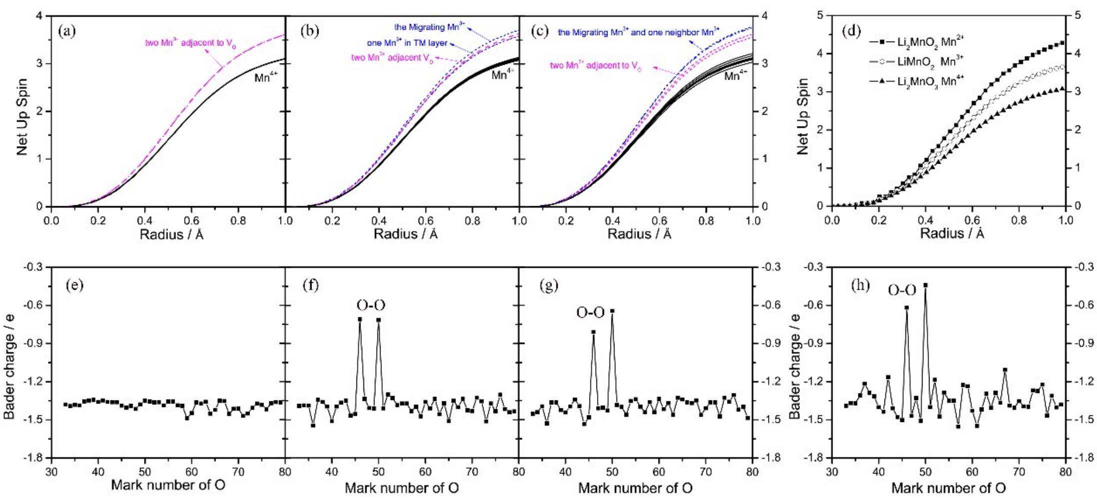

Fig. 3S The net up spin of all Mn atoms (a-c) and the Bader charge of all O atoms (e-f) for snapshot *a*, *f* and *i* shown in Fig. 3, respectively; The net up spin of Mn in Li_2MnO_2, $LiMnO_2$ and Li_2MnO_3 (d); atomic Bader charge of O (h) for snapshot *h* in Fig. 3.

3. FPMD simulation

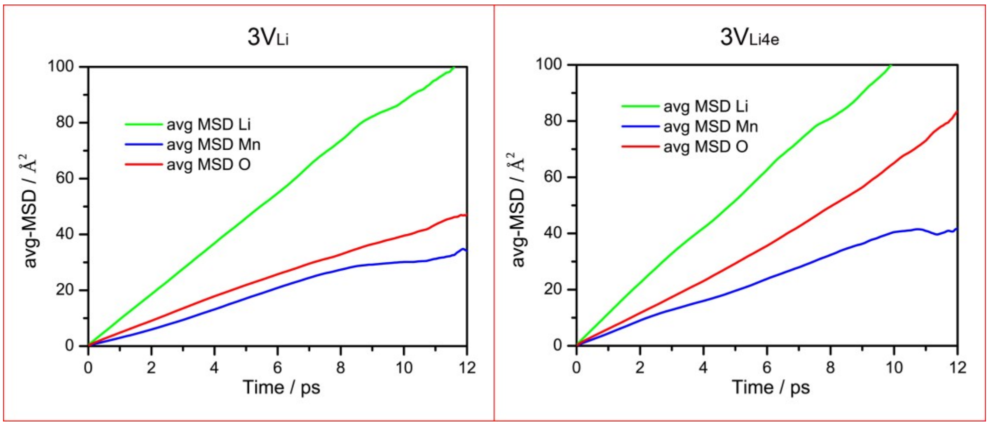

Fig. 4S MSDs of atoms when tree local Li atoms are extracted from the Li layer (denoted as $3V_{Li}$) and two from the Li layer while the last one from the TM layer (denoted as $3V_{Li4e}$) of a perfect Li_2MnO_3 with U_{eff}=4.9 eV at 3000K. Whether the third Li atom is extracted from the Li layer or from the Mn layer, both the Mn and O atoms move intensely. This means that severe deficiency of the local Li ions may finally lead to obvious structural changes, and even local collapse of the structure.

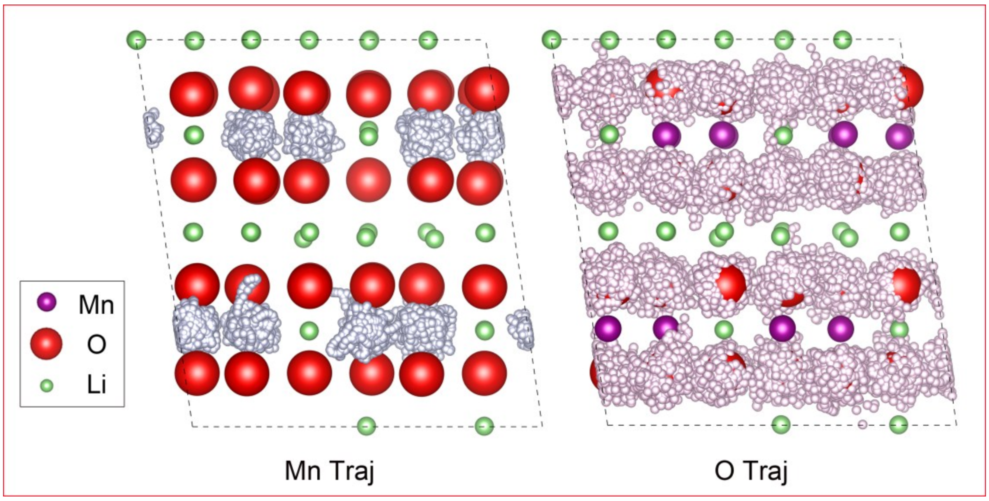

Fig. 5S Trajectories of Mn and O in the structure with one V_O defect with U_{eff} = 4.0 eV at 3000K. In this case, one O vacancy cannot lead to the Mn migration into the Li layer in V_O-Li_2MnO_3, different from the result obtained from U_{eff} = 4.9 eV due to the weak calibration effect of Hubbard U (4.0 eV) for Mn-3d electrons.

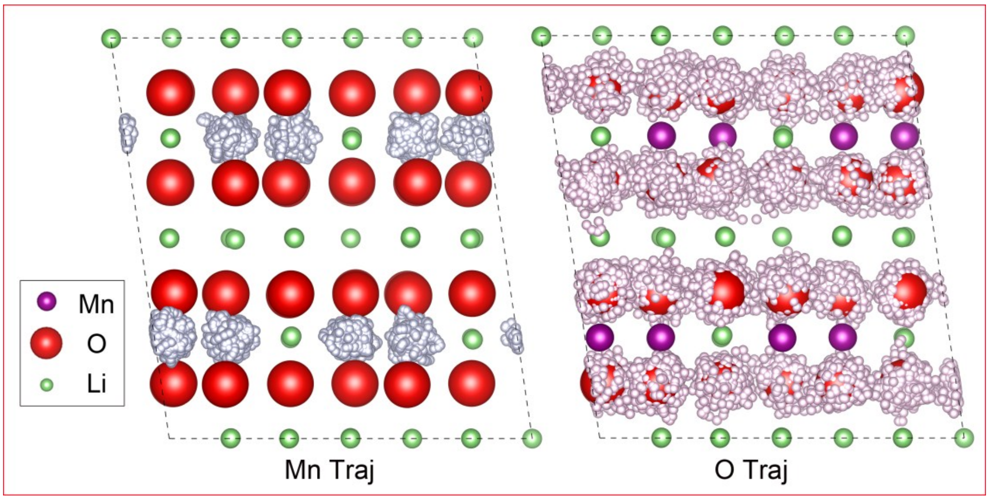

Fig. 6S Trajectories of Mn and O in the structure with one V_{Li} defect (V_{Li}-Li_2MnO_3) with U_{eff} = 4.0 eV at 3000K. In this case, one Li vacancy in the cell cannot lead to the Mn migration into the Li layer in V_{Li}-Li_2MnO_3, agreeing with the result obtained from U_{eff} = 4.9 eV.

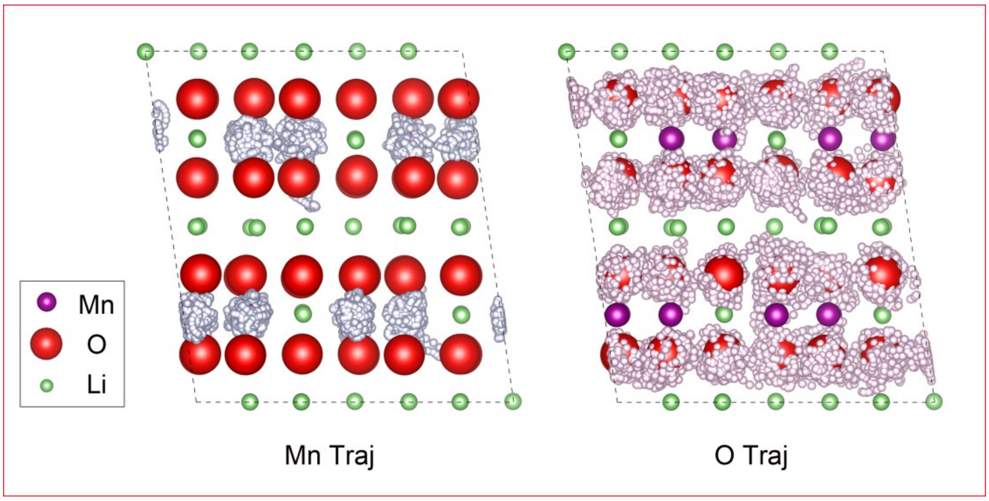

Fig. 7S Trajectories of Mn and O in the structure with two V_{Li} defects ($2V_{Li}$-Li_2MnO_3) with U_{eff} = 4.0 eV at 3000K. In this case, two Li vacancies in the cell cannot lead to the Mn migration into the Li layer in $2V_{Li}$-Li_2MnO_3 due to the weak calibration effect of Hubbard U.

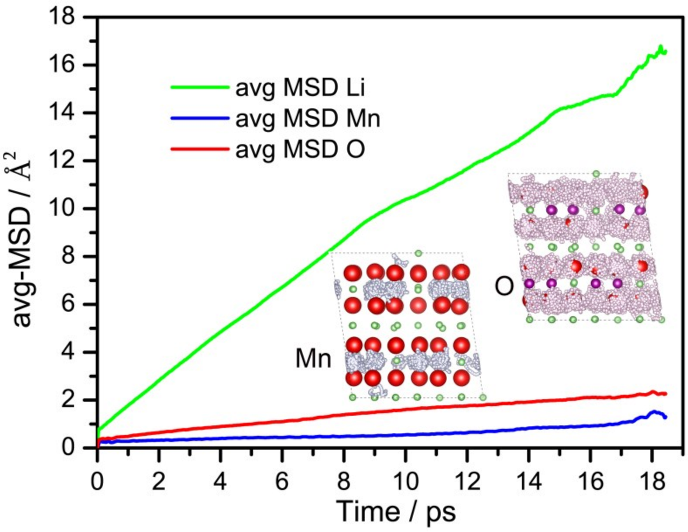

Fig. 8S MSDs of atoms and Trajectories of Mn and O in the structure with one V_{Li} and one V_O defect ($V_{Li}V_O$-Li_2MnO_3) with U_{eff} = 4.0 eV at 3000K. In this case, one local O vacancy plus one Li vacancy in the cell can lead to Mn migration into the Li layer, in good agreement with the result obtained from U_{eff} = 4.9 eV.

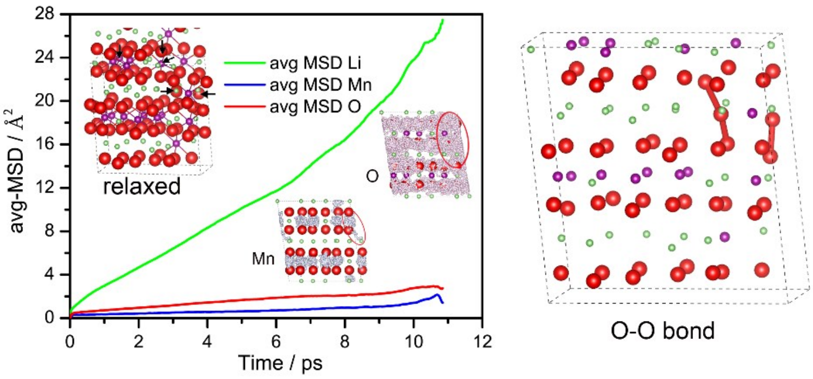

Fig. 9S MSDs of atoms and Trajectories of Mn and O in the structure with $3V_{Li}$ defect with U_{eff} = 4.0 eV at 3000K. Inset of the left picture displays the Mn-O bonds and picture on the right show the O-O bonds in the final relaxed structure. Mn atoms denoted by arrows have CN=5 and O atoms denoted are not bonded to Mn but to Li. Herein, the threshold for bonding lengths of Mn-O and O-O are defined as 2.7 and 1.7 Å, respectively.

Mn migration into the Li layer is observed and the surrounding O atoms move vigorously when the third Li atom is removed from the Li layer (Fig. 9S) but the structure is not changed too severely compared with the result from U_{eff} = 4.9 eV. The final equilibrium structure indicates that the coordination number of the Mn atom in the Li layer is six while that of some Mn atoms in the Mn layer is five. Oxygen is found in the Li layer in the final equilibrium structure. In addition, one O atom is found disconnected with any Mn atoms in the MnO_6 block (but bonded to Li). These may respond to the oxygen evolution. Three O-O bonds are found with lengths of 1.38, 1.41 and 1.59 Å, respectively.

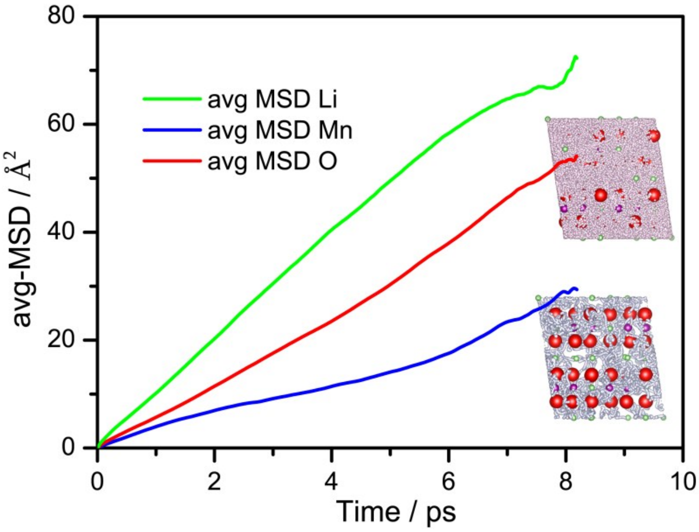

Fig. 10S MSDs of atoms and Trajectories of Mn and O in the structure with $3V_{Li4e}$ defect with U_{eff} = 4.0 eV at 3000K. Mn migration into Li layer is observed when the third Li atom is extracted from the Mn layer. And all the atoms in the lattice are found migrating too severely that the local structure and volume may change a lot, leading to local collapse.

4. Li diffusion

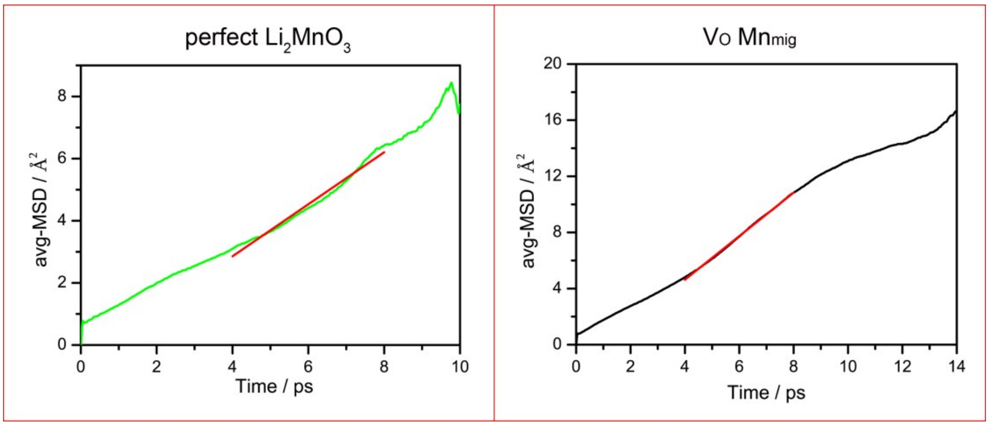

Fig. 11S MSDs of Li in the perfect Li_2MnO_3 and the structure with one V_O defect after Mn migrate into the Li layer at T=3000 K. Within the simulating time, the Mn atom stays in the Li layer of the Li_2MnO_3 with V_O and Mn_{Li4e} defects.

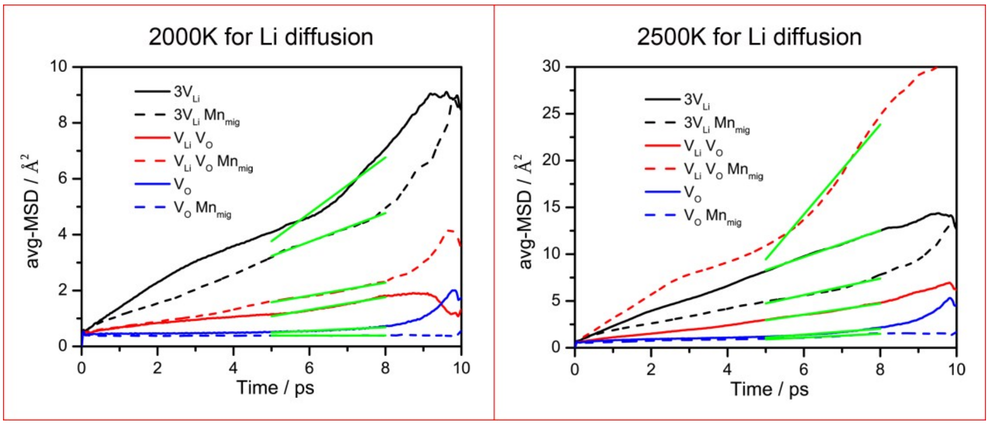

Fig. 12S Linear least squares fitting to the slope of MSDs for Li before and after Mn migration into the Li layer at 2000 and 2500 K.

Table 2S. Lithium diffusion coefficient D ($\times 10^{-9}$ m^2s^{-1}) obtained by linear least squares fitting of the MSDs at 2000K and 2500 K.

T / K	$D(3V_{Li})$	$D(3V_{Li},Mn_{mig})$	$D(V_O)$	$D(V_O,Mn_{mig})$	$D(V_{Li}V_O)$	$D(V_{Li}V_O,Mn_{mig})$
2000	1.66597	0.8534	0.10627	0.0019	0.37995	0.3893
2500	2.36297	1.47328	0.52667	0.33347	0.99453	8.00677

Reference

1. R. Xiao, H. Li, L. Chen, *Chem. Mater.* **2012**, *24*, 4242.